HEPATOBILIARY-PANCREAS

MRI for characterization of benign hepatocellular tumors on hepatobiliary phase: the added value of in-phase imaging and lesion-to-liver visual signal intensity ratio

P. Lebert[1] · M. Adens-Fauquembergue[1] · M. Azahaf[1] · V. Gnemmi[2] · H. Behal[3] · A. Luciani[4] · O. Ernst[1]

Abstract

Objectives To evaluate the lesion-to-liver visual signal intensity ratio (SIR) before and at the hepatobiliary phase MRI (HBP-MRI) after gadobenate dimeglumine (Gd-BOPTA) injection, using several T1-weighted images (T1-WI), for the characterization of benign hepatocellular lesions.

Methods Patients with histologically proven focal nodular hyperplasia (FNH) and hepatocellular adenoma (HCA), who underwent Gd-BOPTA-enhanced HBP-MRI from 2009 to 2017, were retrospectively identified. The lesion-to-liver SIR was visually assessed by two radiologists on HBP (post-HBP analysis) and compared with that of unenhanced sequences (pre/post-HBP analysis) on T1-WI in-phase (T1-IP), out-of-phase (T1-OP), and fat suppression (T1-FS). Lesions were classified as hyper-, iso-, or hypointense on post-HBP, and as decreasing, stable, or increasing SIR on pre/post-HBP analyses. The performance of the different T1-WI sequences for the diagnostic of FNH was evaluated on post-HBP analysis.

Results Twenty-nine FNHs and 33 HCAs were analyzed. On post-HBP analysis, FNHs appeared hyper-/isointense in 89.7% of all T1-WI. HCAs appeared hypointense in 93.9%, 63.6%, and 69.7% of T1-IP, T1-OP, and T1-FS, respectively. FNHs exhibited an increasing SIR in 55.2–58.6%, a stable SIR in 44.8–58.6%, and a decreasing SIR in 0%, whereas HCAs exhibited a decreasing SIR in 66.7–93.9%, a stable SIR in 6.1–33.3%, and an increasing SIR in 0% ($p < 0.0001$). The specificity of T1-IP was significantly higher than that of T1-OP ($p = 0.015$) and T1-FS ($p = 0.042$).

Conclusion T1-IP is the most reliable sequence due to misleading tumor/liver signal ratio in the case of fatty liver when using T1-FS or T1-OP. The pre/post-HBP lesion-to-liver SIR is accurate to classify benign hepatocellular lesions and contributes to avoid biopsy.

Key Points

• *The T1-weighted images in-phase should be systematically included in the HBP-MRI protocol, as it is the most reliable sequence especially in the case of fatty liver.*

• *The comparison between lesion-to-liver signal intensity ratios on unenhanced and at the hepatobiliary phase sequences is useful to classify benign hepatocellular lesions in three categories without misclassification: FNH (increasing signal intensity ratio), HCA (decreasing signal intensity ration), and indeterminate lesions (stable signal intensity ratio).*

Keywords Focal nodular hyperplasia · Gadobenate dimeglumine · Hepatocellular adenoma · Liver · Magnetic resonance imaging

✉ P. Lebert
plebert17@gmail.com

1 Department of Gastrointestinal Imaging, Lille University Hospital, Rue Michel Polonovski, 59037 Lille Cedex, France

2 Department of Pathology, Lille University Hospital, avenue Oscar-Lambret, 59037 Lille Cedex, France

3 Department of Biostatistics, Lille University Hospital, avenue Oscar-Lambret, 59037 Lille Cedex, France

4 Groupe Henri Mondor Albert Chenevier, Imagerie Medicale, AP-HP, 94010 Creteil, France

Abbreviations

FNH	Focal nodular hyperplasia
Gd-BOPTA	Gadobenate dimeglumine
Gd-EBO-DTPA	Gadoxetic acid
GRE	Gradient-recalled echo
HCA	Hepatocellular adenoma
HBP	Hepatobiliary phase
HSCAs	Hepatobiliary-specific contrast agents
OATP	Organic anionic transport protein
SIR	Signal intensity ratio
T1-FS	T1-weighted images with fat suppression

T1-IP	T1-weighted images in-phase
T1-OP	T1-weighted image out-of-phase
THRIVE	T1-WI high-resolution isotropic volume examination
VIBE	Volumetric interpolated breath-hold examination
WI	Weighted images

Introduction

Focal nodular hyperplasia (FNH) is a frequent benign liver lesion, occurring in 0.6–3% of the population [1, 2]. The main differential in patients without chronic liver disease is the hepatocellular adenoma (HCA) [3–5]. Commonly, both FNHs and HCAs are incidentally discovered [6, 7]. However, the management is quite different: FNH requires no follow-up [8], while HCA may lead to surgery, according to the risk of spontaneous bleeding and malignant transformation, depending on molecular subtype and size [4, 9, 10].

Thus, an accurate and confident diagnosis is mandatory, and liver MRI is the most reliable imaging tool [9–11]. The conventional MRI reaches a specificity close to 100% for the diagnosis of FNH when five features are present [1, 9, 12–14]: isointensity in T1- and T2-weighted images (WI), typical central scar (that appears hyperintense in T2-WI, hypointense at the arterial phase, and hyperintense at the delayed phase), homogeneity (excepting the central scar), strong arterial enhancement that vanishes at the delayed phase without any washout, and absence of a capsule [1, 9, 14]. However, 21% of FNHs do not exhibit all these typical features, and differentiation from HCA can be challenging [1, 9, 11–13]. Biopsy remains the gold standard in such cases, but exposes patients to bleeding, even if the risk is low [6, 15–17].

Several reports have shown the added value of the two available hepatobiliary-specific contrast agents (HSCAs), gadobenate dimeglumine (Gd-BOPTA) and gadoxetic acid (Gd-EOB-DTPA) [10, 11, 18–21]. Both combine an extracellular distribution followed by a partial uptake of hepatocytes (approximately 3–5% with Gd-BOPTA and 50% with Gd-EOB-DTPA), allowing hepatobiliary phase (HBP) imaging [22, 23]. FNHs generally exhibit iso- or hyperintensity on HBP images, probably due to the biliary proliferation and the overexpression of membrane transporters (such as organic anionic transport protein [OATP] 1) [22, 23], whereas HCAs are typically hypointense compared with the liver parenchyma on HBP images [11, 12, 24]; however, these results still do not reach a 100% specificity: 3% of the FNHs appeared hypointense in HBP images [12]. Hyperintense HCAs on HBP have also been described [25]. These overlapping findings on HBP images remain problematic and might sometimes be related to technical considerations or liver steatosis [22].

HPB image acquisition can be made with different T1-WI techniques including chemical shift and fat suppression (T1-FS) sequences [26]. Steatosis and nonalcoholic fatty liver disease, which become more and more frequent in the Western population [27], can greatly modify the perception of the signal of the lesions on these sequences.

The purpose of this study was to evaluate the lesion-to-liver visual signal intensity ratio (SIR) before and at the hepatobiliary phase MRI (HBP-MRI) after Gd-BOPTA injection, using several T1-weighted images (T1-WI), for the characterization of benign hepatocellular lesions.

Materials and methods

Population

The study coordinator retrospectively retrieved the pathology reports of 32 asymptomatic patients with one or more hepatic nodules such as FNH or HCA who underwent Gd-BOPTA-enhanced HBP-MRI in two tertiary referral centers between April 2009 and January 2017.

The standard of reference was the histological diagnosis, obtained in all patients by biopsy or surgery. In patients with multiple nodules, the diagnosis was reached only on one lesion and was extended to all the other lesions with the same features on all MRI sequences. A maximum of three lesions per patient was selected.

The histological distinction between FNH and HCA was based on routine stains (hematoxylin-eosin-saffron and trichrome) according to the classical criteria [28] and, when necessary, on the glutamine synthetase immune-staining. A biopsy was also performed in the liver parenchyma to rule out cirrhosis, hepatitis, or iron overload and to allow the diagnosis and the severity of steatosis when present. We did not include patients with incomplete MRI or with lesions less than 10 mm in diameter. Our Institutional Review Board approved this retrospective study and the requirement for informed consent was waived.

Image acquisition

The MRI examinations were performed on an Ingenia 1.5 T (Philips Healthcare) or an Avanto 1.5 T (Siemens Healthineers), and all protocols used T1-, T2-, and diffusion-weighted images, multiphase contrast enhancement sequences (including arterial, portal, and delayed phases). HBP-MRI images were acquired at least 90 min after Gd-BOPTA injection. We performed three different T1-WI with the same parameters on the unenhanced and the HBP sequences: gradient-recalled echo (GRE) in-phase (T1-IP) and out-of-phase (T1-OP) T1-WI, and T1-WI with fat suppression (T1-FS). T1-FS were T1-WI high-resolution isotropic volume examination (THRIVE)

or volumetric interpolated breath-hold examination (VIBE). The MRI parameters of each T1-weighted sequence are reported in Table 1.

Gd-BOPTA (MultiHance; Bracco Diagnostic Inc.) was administered at a 0.1 mL/kg dose (0.05 mmol/kg) body weight as a single intravenous bolus injection followed by a 10-mL saline flush.

Image analysis

All MRIs were reviewed independently by two radiologists who were not involved in patient selection and were blinded to the final diagnosis (observer 1 and observer 2, with 5 and 2 years of experience with abdominal imaging, respectively).

The study coordinator first selected the lesions and showed them to the reviewers on the arterial phase MRI. Then, the two observers performed two different analyses: (1) The post-HBP analysis corresponded to the visual comparison between the signal intensity of the lesion and that of the surrounding liver only at the HBP, called post-HBP lesion-to-liver SIR; (2) The pre/post-HBP analysis corresponded to the visual analysis of the evolution of the lesion-to-liver SIR between the unenhanced and the HBP sequences, called pre/post-HBP lesion-to-liver SIR. For both analyses, the signal intensity of the lesions and the liver was assessed visually on each T1-WI (IP, OP, and FS). When the lesions exhibited heterogeneous enhancement, the signal of most of the lesion (more than 50%) was taken into account. On post-HBP analysis, lesions were classified as hypointense, isointense, or hyperintense. On pre/post-HBP analysis, lesions were classified with a 3-point scale (decreasing SIR, stable SIR, or increasing SIR). A consensus reading was performed with a third observer (observer 3, with 25 years of experience in abdominal imaging) in cases of disagreement.

Observer 3 also performed an evaluation of some conventional MRI features for all lesions, which included the following: lack of a central scar, hypointense scar in T2-WI or on the delayed phase, signal heterogeneity (in exception of the central scar), fat content (characterized by a signal dropout on chemical shift T1-WI), delayed persistent enhancement, portal or delayed hypointensity, and delayed capsule. These features, so-called atypical features, are generally considered unusual for the MRI diagnosis of FNH [1, 9, 13, 14]. The presence of these signs does not allow for differentiation between FNH and HCA on MRI, explaining why they are specifically studied.

Statistical analysis

Qualitative parameters are expressed in frequencies and percentages. The comparison between the pre/post-HBP lesion-to-liver SIR of the FNHs and the HCAs was performed by a chi-squared test. This test was also used to compare the misclassification rates (false negative and false positive) of the post-HBP lesion-to-liver SIR in patients with and without steatosis in each T1-WI.

The performance of the three T1-WI for the diagnosis of FNH was compared by a generalized linear mixed model. The interobserver agreement between observers 1 and 2 was assessed using a weighted kappa coefficient on all lesions and all T1-WI for the pre/post-HBP lesion-to-liver SIR. Statistical testing was performed at the two-tailed α level of 0.05. Data were analyzed using the SAS software package, release 9.4 (SAS Institute Inc.).

Results

Population

Eighty-one lesions were identified in 44 patients, and 19 lesions in 12 patients were excluded for the following reasons: incomplete MRI ($n = 8$) or lesion diameter less than 10 mm ($n = 11$). A total of 62 lesions (29 FNHs and 33 HCAs) in 32 patients (25 female and 7 male, with a mean age of 39 years) were analyzed. Sixteen patients exhibited multiple lesions, and 2 had both FNH and HCA (with histological evidence for each type of lesion). The diagnosis was based on histological analysis in 34 lesions (biopsy, $n = 25$; surgery, $n = 9$). The remaining 28 lesions have been confirmed by the standard expressed in the methods section as "In patients with multiple nodules, the diagnosis was reached only on one lesion and was extended to all the other lesions with the same features on all MRI sequences". Thirteen patients had steatosis on their liver sample. Table 2 reports the main characteristics of the study population.

Table 1 MRI sequences parameters. The same parameters were used for the T1-weighted images performed before Gd-BOPTA injection and at the hepatobiliary phase

	Philips Ingenia 1.5 T				Siemens Avanto 1.5 T			
	TR	TE	Flip angle	Slice thickness	TR	TE	Flip angle	Slice thickness
GRE IP and OP T1-WI	161 ms	2–4 ms	75°	7 mm	121 ms	2.38–4.76 ms	70°	5 mm
VIBE or THRIVE T1-WI	3.8 ms	1.77 ms	16°	4 mm	3.31 ms	1.25 ms	15°	3 mm

T, tesla; *TR*, repetition time; *TE*, echo time; *GRE*, gradient-recalled echo; *IP*, in-phase; *OP*, out-of-phase; *WI*, weighted images; *VIBE*, volumetric interpolated breath-hold examination; *THRIVE*, T1-weighted high-resolution isotropic volume

Table 2 Patient population

	29 FNHs in 19 patients	33 HCAs in 15 patients
Age (years) [mean ± SD (range)]	40.4 ± 9.6 (20–56)	37.7 ± 11.4 (22–60)
Female/male ratio	13/6	14/1
Number of analyzed lesions per patient	12 solitary FNHs 12 multiple FNHs in 5 patients 5 FNHs in association with HCA in 2 patients	4 solitary HCAs 27 multiple HCAs in 9 patients 2 HCAs in association with FNH in 2 patients
Maximum lesion diameter (mm)	33.9 ± 15.3 (12–85)	36.8 ± 27.8 (10–115)
Diagnostic confirmation	17 percutaneous biopsies 2 surgical resections 10 on an identical MRI signal	8 percutaneous biopsies 7 surgical resections 18 on an identical MRI signal
HCA morphological and pathological specificities	NA	17 inflammatory HCAs 2 HNF-1α inactivated HCAs 3 β-catenin mutated HCAs 11 unclassified HCAs
Liver steatosis	$n = 7$ (36.8%)	$n = 7$ (46.7%)

FNH, focal nodular hyperplasia; *HCA*, hepatocellular adenoma; *MRI*, magnetic resonance imaging; *NA*, not applicable

Analyses 1 and 2 (Table 3)

On the post-HBP analysis, 26 FNHs (89.7%) were hyper- or isointense on all T1-WI (Fig. 1), whereas 3 (10.3%) were hypointense. HCAs were hypointense in 31 cases (93.9%) on T1-IP, 21 cases (63.6%) on T1-OP, and 23 cases (69.7%) on T1-FS (Figs. 2 and 3), whereas they were hyper- or isointense in 2 cases (6.1%) on T1-IP, 12 cases (36.4%) on T1-OP, and 10 cases (30.3%) on T1-FS.

On the pre/post-HBP analysis, none of the 29 FNHs (0%) exhibited a decreasing SIR on all T1-WI. The SIR was increasing in 16 (55.2%), 17 (58.6%), and 17 (58.6%) of the FNHs on T1-IP, T1-OP, and T1-FS respectively. The T1-IP, T1-OP, and T1-FS showed a stable SIR in 13 (44.8%), 12 (41.4%), and 12 (41.4%) of the 29 FNHs respectively (Fig. 4). None of the 33 HCAs (0%) exhibited an increasing SIR on all T1-WI. The SIR was decreasing in 31 (93.9%), 22 (66.7%), and 28 (84.8%) of the HCAs on T1-IP, T1-OP, and T1-FS respectively. The T1-IP, T1-OP, and
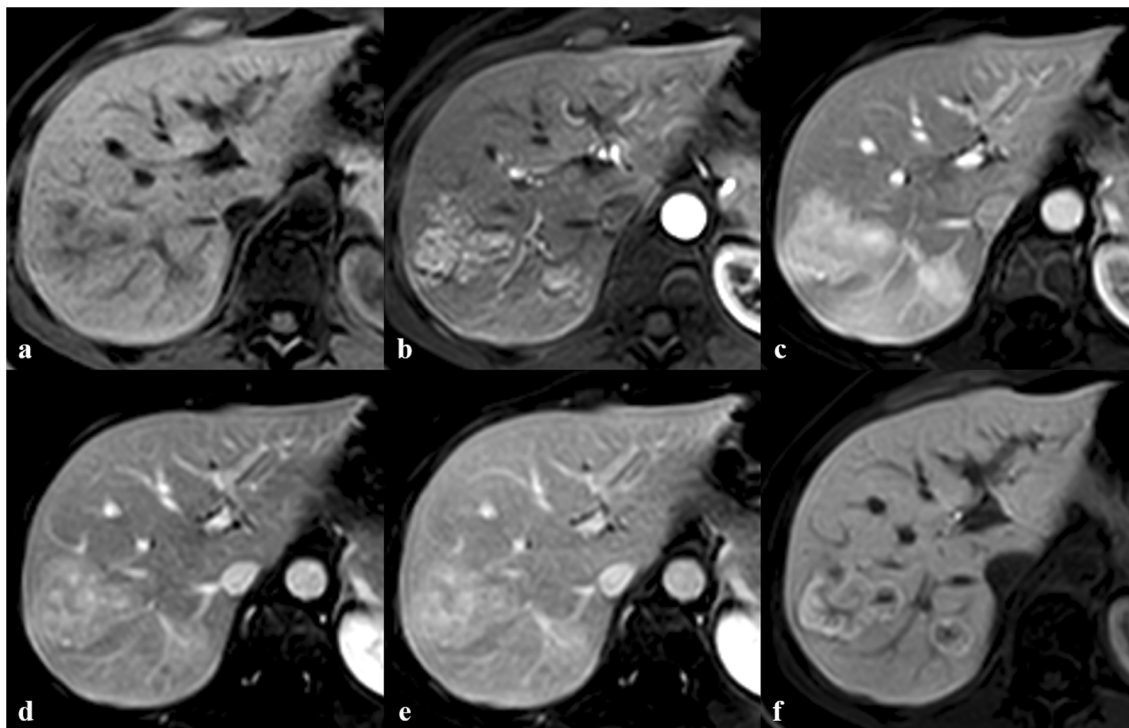

Fig. 1 Multiple FNHs in a 38-year-old female. The multiphase contrast enhancement MRI (**b**, **c**, **d**, and **e**) shows nodules in the right liver that exhibit a marked gadolinium uptake at the arterial phase (**b** and **c**) and tend to be isointense at the delayed phase (**e**). The nodules are hyperintense at the hepatobiliary phase (**f**) with an increasing signal intensity ratio in comparison with the unenhanced phase (**a**)
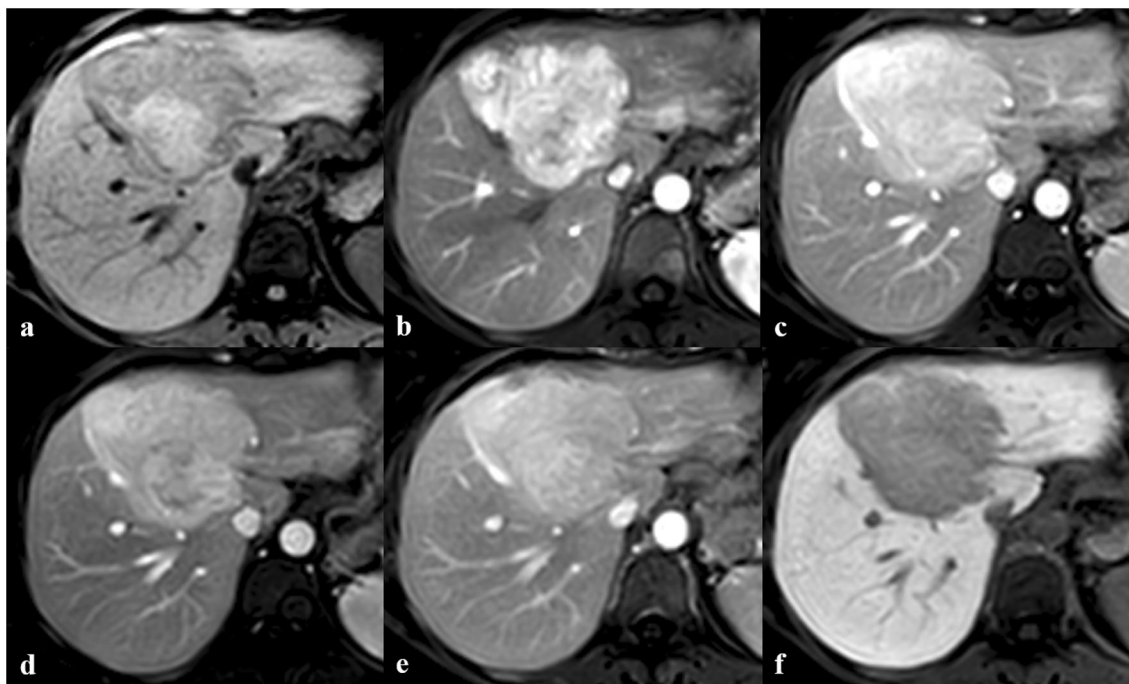
Fig. 2 Inflammatory HCA in a 30-year-old female. The unenhanced sequence (**a**) shows a heterogeneous nodule in the segment IV. The nodule exhibits a marked gadolinium uptake at the arterial phase (**b** and **c**) and is still hyperintense at the portal (**d**) and delayed (**e**) phases. The hepatobiliary phase (**f**) shows a hypointense nodule and a decreasing signal intensity ratio compared with the unenhanced phase (**a**)

T1-FS showed a stable SIR in 2 (6.1%), 11 (33.3%), and 5 (15.2%) of the 33 HCAs respectively.

The stable SIR lesions accounted for 24.2% ($n = 15$), 37.1% ($n = 23$), and 27.4% ($n = 17$) of the lesions on T1-IP, T1-OP, and T1-FS, respectively. In these stable SIR lesions, 13 of 15 (86.7%), 12 of 23 (52.2%), and 12 of 17 (70.6%) were FNHs on T1-IP, T1-OP, and T1-FS, respectively. The pre/post-HBP lesion-to-liver SIR was significantly different between HCAs and FNHs on all T1-WI ($p < 0.0001$).

On T1-IP, the post-HBP lesion-to-liver SIR classified 28 nodules as iso- or hyperintense and 34 nodules as hypointense, with 5 misclassifications (2 HCAs were iso- or hyperintense and 3 FNHs were hypointense). On T1-FS, the post-HBP lesion-to-liver SIR classified 36 nodules as iso- or hyperintense and 26 nodules as hypointense, with 13 misclassifications (10 HCAs were iso- or hyperintense and 3 FNHs were hypointense). On the other hand, the pre/post-HBP lesion-to-liver SIR classified 16 nodules as increasing SIR
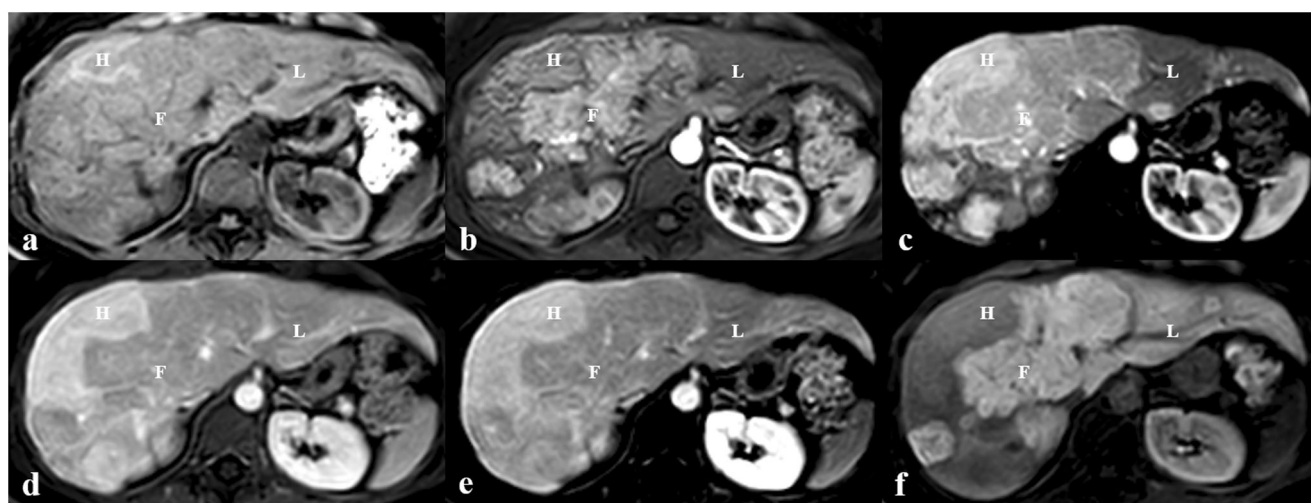

Fig. 3 Inflammatory HCA and multiple FNHs in a 41-year-old female. The multiphase contrast enhancement MRI (**b**, **c**, **d**, and **e**) shows multiple nodules in the right lobe, H corresponding to an inflammatory HCA and F to an FNH. The normal liver is noted (L). The hepatobiliary phase (**f**) shows that H is hypointense and F slightly hyperintense compared with the normal liver and to the unenhanced phase (**a**)

Table 3 Results of post-HBP and pre/post-HBP analyses

				FNH	HCA
Post-HBP analysis	T1-IP	Hyperintense		9 (31%)	0 (0%)
		Isointense		17 (58.6%)	2 (6.1%)
		Hypointense		3 (10.3%)	31 (93.9%)
	T1-OP	Hyperintense		16 (55.2%)	8 (24.2%)
		Isointense		10 (34.5%)	4 (12.1%)
		Hypointense		3 (10.3%)	21 (63.6%)
	T1-FS	Hyperintense		12 (41.4%)	0 (0%)
		Isointense		14 (48.3%)	10 (30.3%)
		Hypointense		3 (10.3%)	23 (69.7%)
Pre- and post-HBP analysis	T1-IP	Increasing SIR		16 (55.2%)	0 (0%)
		Stable SIR		13 (44.8%)	2 (6.1%)
		Decreasing SIR		0 (0%)	31 (93.9%)
	T1-OP	Increasing SIR		17 (58.6%)	0 (0%)
		Stable SIR		12 (41.4%)	11 (33.3%)
		Decreasing SIR		0 (0%)	22 (66.7%)
	T1-FS	Increasing SIR		17 (58.6%)	0 (0%)
		Stable SIR		12 (41.4%)	5 (15.2%)
		Decreasing SIR		0 (0%)	28 (84.8%)

HBP, hepatobiliary phase; *FNH*, focal nodular hyperplasia; *HCA*, hepatocellular adenoma; *T1-IP*, T1-weighted images in-phase; *T1-OP*, T1-weighted images out-of-phase; *T1-FS*, T1-weighted images with fat suppression; *SIR*, signal intensity ratio

and 31 nodules as decreasing SIR, without misclassification in all T1-WI. Fifteen nodules remained indeterminate.

Evaluation of the conventional MRI features

In all 62 lesions, the lack of a central scar was the most common atypical feature ($n = 52$, 84%), followed by signal heterogeneity ($n = 25$, 40%), a delayed persistent enhancement ($n = 9$, 15%), a delayed hypointensity ($n = 4$, 6%), fat content ($n = 3$, 5%), and a delayed capsule ($n = 2$, 3%). The lack of a central scar was the only atypical feature in 24 lesions (39%), 12 FNHs and 12 HCAs. Only three nodules exhibited no atypical features.

Considering the 16 increasing SIR lesions on T1-IP, 1 (6%) had no atypical features, 9 (56%) had only one atypical feature (7 lack of a central scar, 2 delayed persistent enhancement), and 6 (38%) had two or more atypical features. All these increasing lesions were FNHs.

Considering the 31 decreasing SIR lesions on T1-IP, 13 (42%) had only one atypical feature (12 lack of a central scar, 1 delayed persistent enhancement) and 18 (58%) had two or more atypical features. All these decreasing lesions were HCAs.

Considering the 15 stable SIR lesions on T1-IP, 2 (13%) had no atypical features and were FNHs. Nine stable SIR lesions (60%) had only one atypical feature (5 lack of a central scar, 3 signal heterogeneity, and 1 delayed persistent

enhancement) and were all FNHs. Four stable SIR lesions (27%) exhibited two or more atypical features. These 4 lesions were 2 FNHs and 2 HCAs.

Comparison between the three T1-WI on the post-HBP analysis (Tables 4 and 5)

The performance parameters of each T1-WI were calculated for the FNHs' diagnosis on post-HBP analysis. The specificity of the T1-IP was significantly higher than that of the T1-OP ($p = 0.015$) or the T1-FS ($p = 0.042$).

A misclassification rate (false negative and false positive) was calculated for each T1-WI on the post-HBP analysis in patients with and without liver steatosis (Table 4), considering that it was frequently the cause of the error (Fig. 5). The misclassification rate of the T1-FS and the T1-OP with steatosis was significantly higher ($p = 0.036$ and $p = 0.008$, respectively). The test could not be performed with the T1-IP because of the low number of errors.

Interobserver correlation

The interobserver agreement for all lesion and all T1-WI on the pre/post-HBP analysis was 0.73 (95% CI, 0.68–0.79), corresponding to a good agreement between observers.

Fig. 4 Solitary FNH in a 33-year-old female. The hepatobiliary phase (**b**) shows a hypointense subcapsular nodule in the segment V. The lesion-to-liver signal intensity ratio is stable or slightly increased compared with the unenhanced phase (**a**)
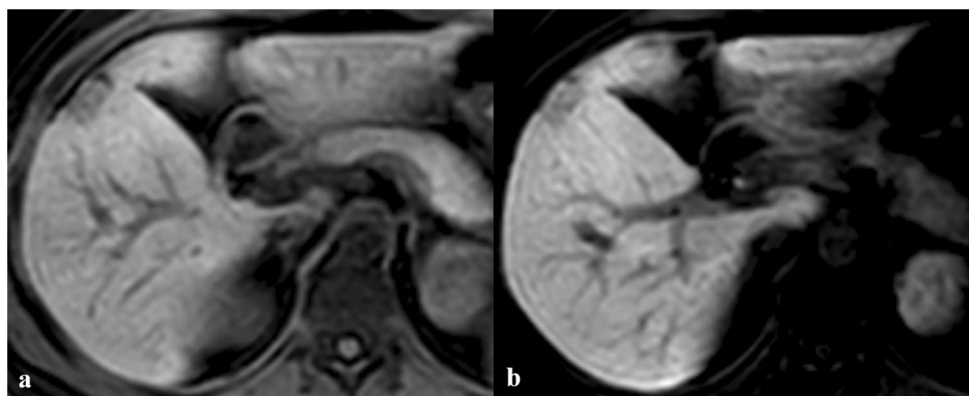
Discussion

Our study highlights the T1-IP on HBP as the most reliable sequence to allow the diagnosis of HCA in the liver with steatosis. Another relevant result is the high added value of the pre/post-HBP lesion-to-liver SIR in the distinction between FNH and HCA in patients without underlying liver disease: no FNH exhibited a decreasing SIR, and no HCA exhibited an increasing SIR between the unenhanced and the HBP. These results suggest that biopsy could be avoided in some cases. However, the pre/post-HBP lesion-to-liver SIR failed to classify the 16 stable SIR lesions. The post-HBP analysis is consistent with the reported literature [11, 12, 16, 17, 20, 21, 24, 29].

In our study, only 3 lesions exhibited all the typical MRI features of FNHs. In all other cases, the conventional MRI features were insufficient to confirm the diagnosis. The HSCAs increased the overall accuracy in diagnosing the hepatocellular lesions up to 96% [11, 12, 20, 21, 29], but some authors reported iso- or hyperintense HCAs on HBP [5, 25, 30]. In our study, 2 HCAs were incorrectly classified as iso- or hyperintense on the post-HBP analysis on the T1-WI IP and 10 on the T1-WI FS. These misclassifications are not acceptable in this young population, given the risk of complications in the case of HCA [31].

Several reasons could explain the iso- or hyperintensity of the HCAs on HBP: first, some HCAs have been reported to

overexpress molecular transporters such as OATP1, which are thought to be involved in Gd-BOPTA uptake [23, 25, 30, 32]. Second, most of the inflammatory HCAs have been described as hyperintense on HBP images due to their pathologic features (such as ductular reaction and sinusoidal dilatation) [5], but in our study, 16 of the 17 inflammatory HCAs were hypointense at the HBP. Laumonier et al [33] pointed out that FNH with sinusoidal dilatation is a misleading entity, which can be confused with the inflammatory HCAs due to overlapping pathologic features. These two entities should no longer be misdiagnosed with the addition of glutamine synthetase immune-staining, showing a characteristic map-like pattern in FNHs [2]. This could be a part of an explanation of the results of the Thomeer study [5], but liver steatosis could also be responsible for the iso- or hyperintense HCA aspect on HBP [3, 22], since the HBP assessment was done on T1-FS sequences in previous studies [5, 6, 24, 25, 30, 34]. In our study, 2 HCAs appeared isointense on T1-IP at the HBP, compared with 10 on the T1-FS. Furthermore, the error rate was significantly higher in fatty livers when evaluating T1-FS and T1-OP. T1-IP showed approximately the same error rate with or without liver steatosis (7.4% vs. 8.6%). These results confirm the role of the steatosis in such a presentation of the HCAs on HBP. Only 1 of the 2 isointense HCAs exhibited a stable SI, and the other one exhibited a decreased SI. Therefore, pre/post-HBP lesion-to-liver SIR showed better efficacy to characterize nodules than the post-HBP lesion-to-

Table 4 Performances of the T1-weighted images for the diagnosis of focal nodular hyperplasia on post-HBP analysis

	Sp	Se	NPV	PPV
T1-IP	93.9%	89.7%	91.2%	92.9%
T1-OP	63.6%	89.7%	87.5%	68.4%
T1-FS	69.7%	89.7%	88.5%	72.2%

T1-IP, T1-weighted images in-phase; *T1-OP*, T1-weighted images out-of-phase; *T1-FS*, T1-weighted images with fat suppression; *Sp*, specificity; *Se*, sensibility; *NPV*, negative predictive value; *PPV*, positive predictive value

Table 5 Impact of the liver steatosis on misclassifications of post-HBP analysis

	Liver steatosis	No liver steatosis	*p* value
T1-WI in-phase	2 (7.4%)	3 (8.6%)	NA
T1-WI out-of-phase	11 (40.7%)	4 (11.4%)	0.008
T1-WI FS	9 (33.3%)	4 (11.4%)	0.036

Data are misclassification numbers, which are false negative (such as iso- or hyperintense HCAs) and false positive (such as hypointense FNHs) of post-HBP analysis, with percentages in parentheses

T1-WI, T1-weighted images; *FS*, fat suppression; *NA*, not applicable
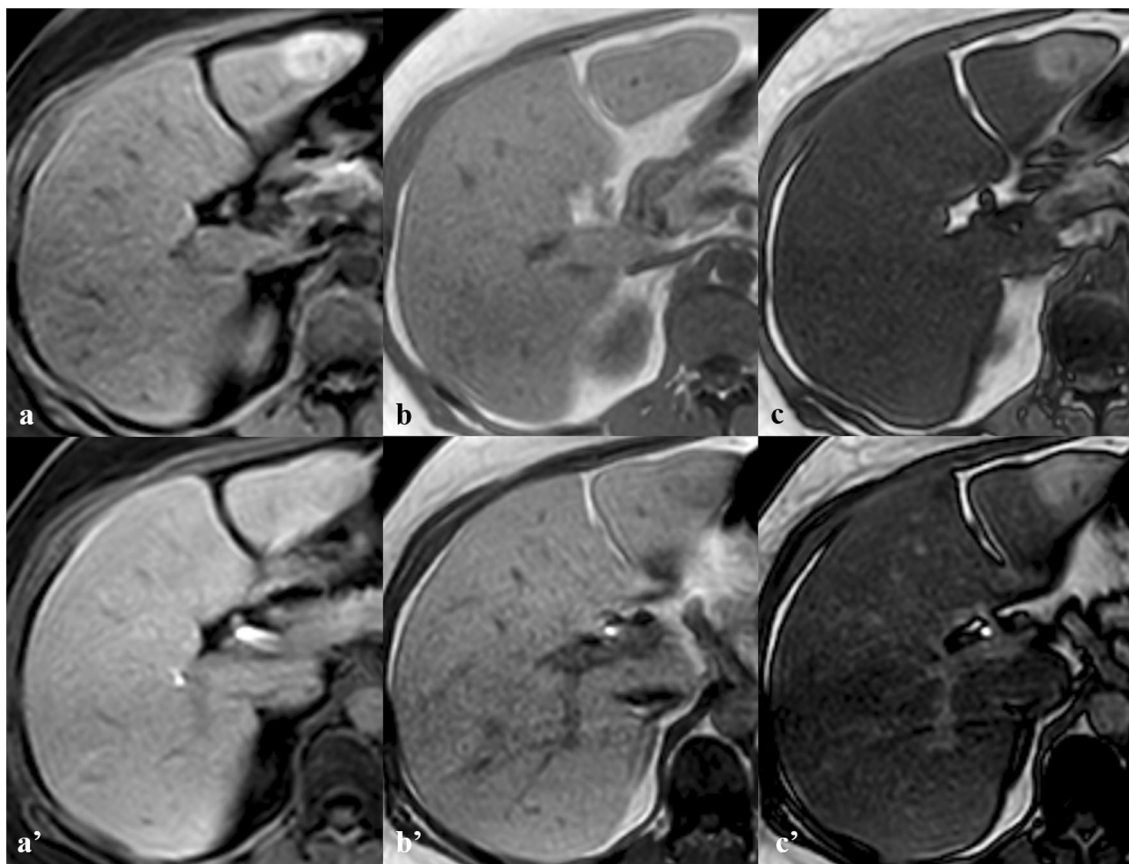
Fig. 5 Inflammatory HCA in a 46-year-old female. T1-FS (**a′**) and T1-OP (**c′**) at the hepatobiliary phase show an iso- or hyperintense nodule in the left lobe, whereas the T1-IP (**b′**) show a hypointense nodule. The nodule was hyperintense on the unenhanced T1-FS (**a**), due to fatty liver steatosis (**b** and **c**), that corresponds to an increasing signal intensity ratio on the pre/post-HBP analysis

liver SIR, suggesting that assessment of the surrounding liver plays a major role in the lesions signal evaluation, especially in fatty livers.

On the other hand, hypointense FNHs on HBP may rarely occur, especially in small lesions (approximately 3%), according to Grazioli et al [12]. In our study, 10.3% of the FNHs appeared hypointense on HBP images, which is more than reported in the literature. This could be explained by a selection bias. We only included histologically proven FNHs, which were, therefore, predominantly atypical FNHs. However, none of the FNHs showed a decreased SIR, which is a new feature. Fujiwara et al [35] showed that the central scar could explain the hypointensity on HBP and could be associated with a rim-accentuated enhancement.

In this study, the pre/post-HBP lesion-to-liver SIR showed a high efficiency for classifying hepatocellular benign lesion in three categories (increasing SIR lesions are FNHs, decreasing SIR lesions are HCAs, and stable SIR lesions are indeterminate) without misclassification. This suggests that the pre/post-HBP lesion-to-liver SIR may help avoid biopsy in increasing SIR lesions, representing more than 50% of all studied FNHs. The evaluation of conventional MRI features showed that indeterminate nodules with a single atypical feature, representing 73% of indeterminate nodules, were all FNHs. This suggests that even more biopsies may be avoided, until about 93% of all studied FNHs (27 of 29 cases).

The main limitation of this study is the selection bias due to the retrospective recruitment on the basis of histologically proven lesions. Therefore, we included more atypical FNHs than in prior studies. The distribution of FNHs and HCAs is also not a representative of the general population. This study focused on benign hepatocellular lesions and did not include hepatocellular carcinoma, which rarely shows a Gd-BOPTA uptake on HBP [36].

Recently, the European Medicines Agency recommended to suspend the Gd-BOPTA marketing authorization due to a potential risk of brain gadolinium retention [37, 38] but maintained its use to liver imaging due to an important diagnostic need [39].

Conclusion

The pre/post-HBP lesion-to-liver SIR has shown high efficiency in classifying benign hepatocellular lesions in three categories without misclassification: increasing, stable, and

decreasing SIR lesions. Increasing SIR lesions are FNHs and decreasing SIR lesions are HCAs. Therefore, a biopsy can be avoided in more than 50% of atypical FNHs. The study also highlights that T1-WI in-phase is the most reliable sequence for the HBP, and it is recommended to include it systematically, as it avoids confusing signal observed with OP and FS in the case of fatty liver.

Compliance with ethical standards

Guarantor The scientific guarantor of this publication is O. Ernst.

Conflict of interest The authors of this manuscript declare no relationships with any companies, whose products or services may be related to the subject matter of the article.

Statistics and biometry One of the authors has significant statistical expertise (H. Behal).

Informed consent Written informed consent was waived by the Institutional Review Board.

Ethical approval Institutional Review Board approval was obtained.

Study subjects or cohorts overlap Some study subjects or cohorts have been previously reported in: Roux et al (2015) Differentiation of focal nodular hyperplasia from hepatocellular adenoma: Role of the quantitative analysis of gadobenate dimeglumine-enhanced hepatobiliary phase MRI. J Magn Reson Imaging JMRI 42(5):1249–58.

Methodology
• Retrospective, diagnostic or prognostic study, performed at two institutions

References

1. Vilgrain V (2006) Focal nodular hyperplasia. Eur J Radiol 58:236–245

2. Bioulac-Sage P, Laumonier H, Rullier A et al (2009) Overexpression of glutamine synthetase in focal nodular hyperplasia: a novel easy diagnostic tool in surgical pathology. Liver Int 29:459–465

3. Laumonier H, Bioulac-Sage P, Laurent C, Zucman-Rossi J, Balabaud C, Trillaud H (2008) Hepatocellular adenomas: magnetic resonance imaging features as a function of molecular pathological classification. Hepatology 48:808–818

4. van Aalten SM, Thomeer MG, Terkivatan T et al (2011) Hepatocellular adenomas: correlation of MR imaging findings with pathologic subtype classification. Radiology 261:172–181

5. Thomeer MG, Willemssen FE, Biermann KK et al (2014) MRI features of inflammatory hepatocellular adenomas on hepatocyte phase imaging with liver-specific contrast agents. J Magn Reson Imaging 39:1259–1264

6. Bieze M, van den Esschert JW, Nio CY et al (2012) Diagnostic accuracy of MRI in differentiating hepatocellular adenoma from focal nodular hyperplasia: prospective study of the additional value of gadoxetate disodium. AJR Am J Roentgenol 199:26–34

7. van Kessel CS, de Boer E, ten Kate FJ, Brosens LA, Veldhuis WB, van Leeuwen MS (2013) Focal nodular hyperplasia: hepatobiliary enhancement patterns on gadoxetic-acid contrast-enhanced MRI. Abdom Imaging 38:490–501

8. European Association for the Study of the Liver (2016) EASL clinical practice guidelines on the management of benign liver tumours. J Hepatol 65:386–398

9. Ronot M, Vilgrain V (2014) Imaging of benign hepatocellular lesions: current concepts and recent updates. Clin Res Hepatol Gastroenterol 38:681–688

10. Neri E, Bali MA, Ba-Ssalamah A et al (2016) ESGAR consensus statement on liver MR imaging and clinical use of liver-specific contrast agents. Eur Radiol 26:921–931

11. Merkle EM, Zech CJ, Bartolozzi C et al (2016) Consensus report from the 7th international forum for liver magnetic resonance imaging. Eur Radiol 26:674–682

12. Grazioli L, Morana G, Kirchin MA, Schneider G (2005) Accurate differentiation of focal nodular hyperplasia from hepatic adenoma at gadobenate dimeglumine-enhanced MR imaging: prospective study. Radiology 236:166–177

13. Ferlicot S, Kobeiter H, van Nhieu JT et al (2004) MRI of atypical focal nodular hyperplasia of the liver: radiology-pathology correlation. AJR Am J Roentgenol 182:1227–1231

14. Khanna M, Ramanathan S, Fasih N, Schieda N, Virmani V, McInnes MDF (2015) Current updates on the molecular genetics and magnetic resonance imaging of focal nodular hyperplasia and hepatocellular adenoma. Insights Imaging 6:347–362

15. Suh CH, Kim KW, Park SH et al (2018) A cost-effectiveness analysis of the diagnostic strategies for differentiating focal nodular hyperplasia from hepatocellular adenoma. Eur Radiol 28:214–225

16. Grieser C, Steffen IG, Kramme IB et al (2014) Gadoxetic acid enhanced MRI for differentiation of FNH and HCA: a single centre experience. Eur Radiol 24:1339–1348

17. Tselikas L, Pigneur F, Roux M et al (2017) Impact of hepatobiliary phase liver MRI versus contrast-enhanced ultrasound after an inconclusive extracellular gadolinium-based contrast-enhanced MRI for the diagnosis of benign hepatocellular tumors. Abdom Radiol (NY) 42:825–832

18. Pirovano G, Vanzulli A, Marti-Bonmati L et al (2000) Evaluation of the accuracy of gadobenate dimeglumine-enhanced MR imaging in the detection and characterization of focal liver lesions. AJR Am J Roentgenol 175:1111–1120

19. Zech CJ, Grazioli L, Breuer J, Reiser MF, Schoenberg SO (2008) Diagnostic performance and description of morphological features of focal nodular hyperplasia in Gd-EOB-DTPA-enhanced liver magnetic resonance imaging: results of a multicenter trial. Invest Radiol 43:504–511

20. McInnes MD, Hibbert RM, Inacio JR, Schieda N (2015) Focal nodular hyperplasia and hepatocellular adenoma: accuracy of gadoxetic acid-enhanced MR imaging–a systematic review. Radiology 277:413–423

21. Suh CH, Kim KW, Kim GY, Shin YM, Kim PN, Park SH (2015) The diagnostic value of Gd-EOB-DTPA-MRI for the diagnosis of focal nodular hyperplasia: a systematic review and meta-analysis. Eur Radiol 25:950–960

22. Roux M, Pigneur F, Calderaro J et al (2015) Differentiation of focal nodular hyperplasia from hepatocellular adenoma: role of the quantitative analysis of gadobenate dimeglumine-enhanced hepatobiliary phase MRI. J Magn Reson Imaging 42:1249–1258

23. Goodwin MD, Dobson JE, Sirlin CB, Lim BG, Stella DL (2011) Diagnostic challenges and pitfalls in MR imaging with hepatocyte-specific contrast agents. Radiographics 31:1547–1568

24. Gupta RT, Iseman CM, Leyendecker JR, Shyknevsky I, Merkle EM, Taouli B (2012) Diagnosis of focal nodular hyperplasia with MRI: multicenter retrospective study comparing gadobenate

dimeglumine to gadoxetate disodium. AJR Am J Roentgenol 199: 35–43

25. Agarwal S, Fuentes-Orrego JM, Arnason T et al (2014) Inflammatory hepatocellular adenomas can mimic focal nodular hyperplasia on gadoxetic acid-enhanced MRI. AJR Am J Roentgenol 203:W408–W414

26. Donato H, França M, Candelária I, Caseiro-Alves F (2017) Liver MRI: from basic protocol to advanced techniques. Eur J Radiol 93: 30–39

27. European Association for the Study of the Liver (EASL), European Association for the Study of Diabetes (EASD), European Association for the Study of Obesity (EASO) (2016) EASL-EASD-EASO Clinical Practice Guidelines for the management of non-alcoholic fatty liver disease. J Hepatol 64(6):1388–1402

28. Bioulac-Sage P, Balabaud C, Wanless I (2010) Focal nodular hyperplasia and hepatocellular adenoma. In: Bosman FT, Carneiro F, Hruban RH, Theise ND (eds) WHO Classification of Tumours of the Digestive System. IARC, Lyon, pp 198–204

29. Grazioli L, Bondioni MP, Haradome H et al (2012) Hepatocellular adenoma and focal nodular hyperplasia: value of gadoxetic acid-enhanced MR imaging in differential diagnosis. Radiology 262: 520–529

30. Yoneda N, Matsui O, Kitao A et al (2012) Beta-catenin-activated hepatocellular adenoma showing hyperintensity on hepatobiliary-phase gadoxetic-enhanced magnetic resonance imaging and over-expression of OATP8. Jpn J Radiol 30:777–782

31. Nault JC, Couchy G, Balabaud C et al (2017) Molecular classification of hepatocellular adenoma associates with risk factors, bleeding, and malignant transformation. Gastroenterology 152:880–894.e886

32. Reizine E, Amaddeo G, Pigneur F et al (2018) Quantitative correlation between uptake of Gd-BOPTA on hepatobiliary phase and tumor molecular features in patients with benign hepatocellular lesions. Eur Radiol 28:4243–4253

33. Laumonier H, Frulio N, Laurent C, Balabaud C, Zucman-Rossi J, Bioulac-Sage P (2010) Focal nodular hyperplasia with major sinusoidal dilatation: a misleading entity. BMJ Case Rep 2010: bcr0920103311

34. Tse JR, Naini BV, Lu DS, Raman SS (2016) Qualitative and quantitative gadoxetic acid-enhanced MR imaging helps subtype hepatocellular adenomas. Radiology 279:118–127

35. Fujiwara H, Sekine S, Onaya H, Shimada K, Mikata R, Arai Y (2011) Ring-like enhancement of focal nodular hyperplasia with hepatobiliary-phase Gd-EOB-DTPA-enhanced magnetic resonance imaging: radiological-pathological correlation. Jpn J Radiol 29: 739–743

36. Narita M, Hatano E, Arizono S et al (2009) Expression of OATP1B3 determines uptake of Gd-EOB-DTPA in hepatocellular carcinoma. J Gastroenterol 44:793–798

37. Dekkers IA, Roos R, van der Molen AJ (2018) Gadolinium retention after administration of contrast agents based on linear chelators and the recommendations of the European Medicines Agency. Eur Radiol 28:1579–1584

38. Runge VM (2017) Critical questions regarding gadolinium deposition in the brain and body after injections of the gadolinium-based contrast agents, safety, and clinical recommendations in consideration of the EMA's pharmacovigilance and risk assessment committee recommendation for suspension of the marketing authorizations for 4 linear agents. Invest Radiol 52:317–323

39. Roux M, Pigneur F, Baranes L et al (2018) Differentiating focal nodular hyperplasia from hepatocellular adenoma: is hepatobiliary phase MRI (HBP-MRI) using linear gadolinium chelates always useful? Abdom Radiol (NY) 43:1670–1681